ISSN: 2692-5397
DOI: 10.33552/MCMS.2022.05.000603
Modern Concepts in Material Science
Iris Publishers

Research Article

Enhancement of the Thermoelectric Properties of Fe_2VAl with the Introduction of Porosity

S Bandaru*[1], O Rapaud[2], F Rouessac[1] and P Jund[1]

[1]*ICGM, Univ. Montpellier, CNRS, ENSCM, Montpellier, France*
[2]*IRCER, UMR-CNRS 7315, France*

***Corresponding author:** S Bandaru, ICGM, Univ. Montpellier, CNRS, ENSCM, Montpellier, France

Received Date: October 26, 2022
Published Date: November 22, 2022

Abstract

Fe_2VAl Heusler-based alloys belong to the category of promising thermoelectric materials but are limited in their use due to their high thermal conductivity. The low ZT values of Fe_2VAl samples could be improved by modifying their morphology and introducing porosity. For this purpose, Fe_2VAl powders were synthesized by mechanical alloying together with different contents of NaCl. Addition of NaCl as a templating agent during milling and its removal resulted in a porosity of around 20% in the nanostructured samples. An enhancement was found in the thermoelectric properties of porous samples. The reduction of the thermal conductivity was attained without affecting the values of the power factor.

Keywords: Porosity; Ball milling; Fe_2VAl, Heusler alloys; Thermoelectric materials

Introduction

The demand for pollution free and sustainable energy sources is gaining in interest as a result of global warming effects and increasing energy costs. Thermoelectric energy converters are of great interest for this purpose as these devices can be utilized in waste heat recovery from various sources like industries, power plants, automobiles, etc... using the Seebeck effect. The efficiency of a thermoelectric material is often estimated by its dimensionless figure of merit ZT (= $S^2\sigma T/\kappa$) which is directly proportional to the electrical conductivity σ, the square of the Seebeck coefficient S and inversely proportional to the thermal conductivity κ. The most successful commercial thermoelectric devices Bi_2Te_3 and PbTe have the drawbacks of high toxicity and high cost of the constitutive elements. This drives to an urgent requirement of efficient and ecofriendly thermoelectric devices. Enhancement of thermoelectric properties can be done in different ways such as doping or introducing nanostructures to the materials in order to reduce κ [1].

Among various thermoelectric materials, Heusler alloys exhibit remarkable thermoelectric properties [2]. Heusler phases are intermetallics with a particular composition and a FCC crystal structure which are categorized in two families: one with the composition 1:1:1 (also known as half-Heuslers) and the other one with the 2:1:1 stoichiometry (full Heuslers). In this last family the Fe_2VAl alloy gained attention due to its semiconducting nature over a wide temperature range up to 1200 K [3,4]. This compound also possesses a high thermoelectric power factor (PF = $S^2\sigma$) at room temperature [5,6]. It is a nonmagnetic semimetal with a sharp pseudogap of 0.1 ~ 0.2 eV at the Fermi level leading to the high values of the PF [7-10]. Several electronic structure calculations conclude to the

existence of a pseudogap at the Fermi level which is also confirmed experimentally by nuclear magnetic resonance (NMR) studies and optical conductivity measurements [11,12]. Very recently, a DFT study taking into account defects and temperature effects, showed an increase of the band gap with temperature. This study reconciles all the available experimental measurements claiming Fe_2VAl to be a semi-metal at low temperature and a semiconductor at high temperature [13] which is beneficial for thermoelectricity. Moreover, a high mechanical strength of around 800 MPa and its resistance to oxidation and corrosion make this alloy suitable for the development of thermoelectric modules [14]. However, the high intrinsic κ value of 28 $W.m^{-1}.K^{-1}$ at 300K, limits the performance of this thermoelectric material and results in low values of ZT [6]. The basic idea of the present work is to improve the ZT by tailoring the microstructure of Fe_2VAl by modifying the morphology and introducing porosity. This can decrease the κ value with the aid of boundary scattering effects increasing the mean free path of the phonons. It is quite challenging to determine if mesoporous samples in the case of Fe_2VAl can modify the transport properties in an auspicious way. Lee et al have studied the effect of nanoscale porosity on SiGe and demonstrated that it will degrade the thermoelectric properties despite the reduction of the the thermal conductivity [15]. However, a study made by Lidorenko et al in the 70's in the case of porous SiGe alloys indicated a possible enhancement in the ZT values using microscale porous structures due to the increase in the ratio of the electrical conductivity to the thermal conductivity by 30% [16]. Recently, an enhancement of ZT at high temperatures is reported in the case of CdO ceramics with randomly distributed micropores [17]. To design nanoscaled and porous Fe_2VAl samples, we have followed a new idea: milling the constituent elements together with NaCl acting as a porogenic additive. We show that a significant enhancement of ZT can be obtained for the samples with a limited porosity. This highlights the fact that the porosity has to be limited and controlled precisely in order to obtain good thermoelectric properties.

Material and Methods

Mechanical alloying of Fe_2VAl alloys was performed by mixing appropriate amounts of Fe (97 %), V (99.7 %) and Fe-Al (99.9 %). All the powders were milled in a Fritsch P5 planetary ball mill with an 80 ml-capacity Cr steel pot and balls with two different ball to powder ratios (BPR) of 10:1 and 13:1. Milling was performed in an Ar atmosphere environment at 400 rpm for 50 h with a 15 min rest every 30 min. To reduce the particle size and to obtain porosity in the samples, 2 wt % and 5 wt % of pure NaCl was added in the pots during milling. NaCl was removed from the powders later by cleaning the powders thoroughly using distilled water which leads to the creation of porosity in the samples.

All the milled Fe_2VAl powders were sintered rapidly using spark plasma sintering (SPS) at the PNF^2 facility in Toulouse, France. All the powders were placed in a graphite mold and sintered at 1273 K under a uniaxial pressure of 60 MPa for 10 min in vacuum. The heating rate was fixed to 100 K/min. The crystallographic structure of the samples was investigated by X-ray diffraction (XRD) using a PANanalytical X'Pert Pro-MPD diffractometer with the Cu K_α radiation. The morphology and the compositional analysis of the samples were studied by using a scanning electron microscope (SEM) FEI Quanta 200 coupled with an energy dispersive X-ray spectroscopy (EDXS). The density of the sintered samples was measured by using Archimedes' principle. The measurements of the Seebeck coefficient and the electrical resistivity were performed with a ZEM-3 ULVAC apparatus. All the specimens used on the ZEM-3 device were shaped into 10×3×3 mm^3 parallelepipeds approximately. In addition, the thermal conductivity was evaluated with the relation $\kappa = \alpha D C_p$ from the thermal diffusivity (α), density (D) and heat capacity (C_p). The measurement of α was implemented by Laser Flash Analysis (Netzsch LFA 427). D was estimated using Archimedes' method. C_p values were obtained from reference [18].

Results and Discussion

Mechanical alloying

The crystallographic peaks of the powders milled with BPRs 10:1 and 13:1 was analyzed by XRD. Irrespective of the different BPRs, the XRD peaks clearly indicate the formation of the A2 phase which is a disordered $L2_1$ Heusler phase without any additional peaks. This clearly indicates that the chosen BPRs are more favourable for crystallizing the powders into the desired $L2_1$ phase after sintering. Moreover, the results are also in very good agreement with the ones obtained for the samples of Mikami et al. [19,20] which are shown in the inset of Figure 1.

The crystallographic analysis of the samples milled together with NaCl was performed after the removal of NaCl and is shown in Figure 2. Since it is difficult to detect the presence of NaCl due to its low content (<1%) in the Fe_2VAl powders (even before washing and even more so after washing) there are no traces of any unwanted peaks in the XRD patterns: the observed peaks clearly indicate the formation of the A2 phase. So, at this stage of the synthesis, it is not possible to detect the presence of NaCl in the diffraction data.

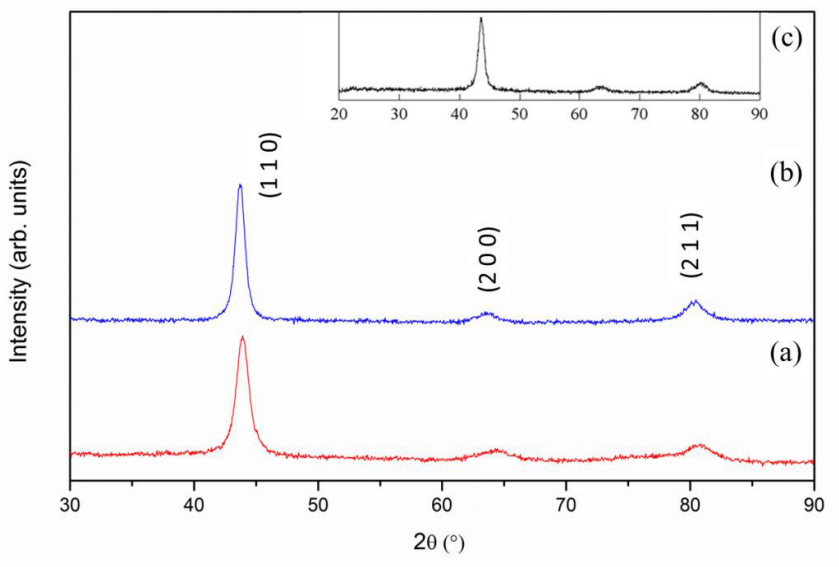

Figure 1: XRD patterns of Fe_2VAl powders with BPR (a) 10:1, (b) 13:1 and (c) Mikami et al [19,20].

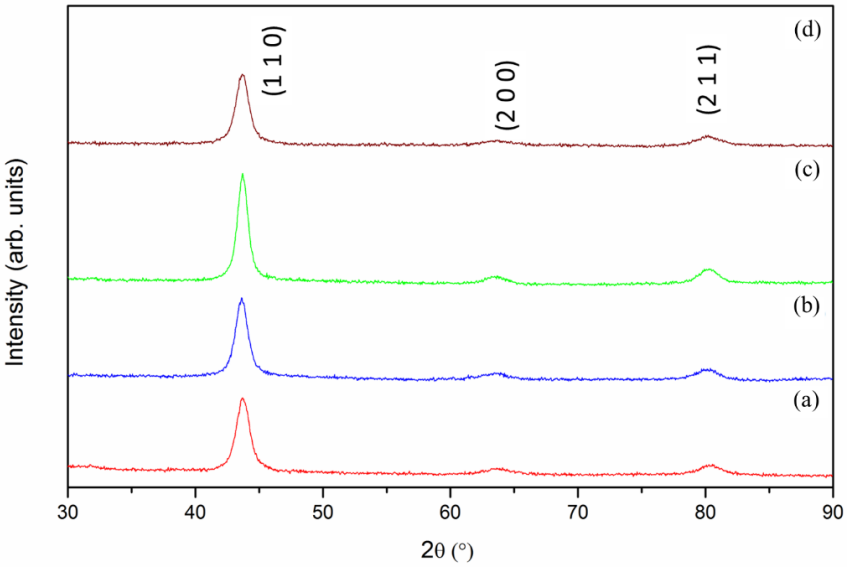

Figure 2: XRD patterns of Fe_2VAl powders after removal of NaCl (a) BPR 10:1 with 2 wt % NaCl, (b) BPR 10:1 with 5 wt % NaCl, (c) BPR 13:1 with 2 wt % NaCl and (d) BPR 13:1 with 5 wt % NaCl.

The morphology of the milled Fe_2VAl powders with BPRs 10:1 and 13:1 is illustrated in Figure 3. The particle size of pure Fe_2VAl is big and around 1-5 μm in the case of 10:1 and 13:1 as shown in Figure 3 (a) and 3 (d). Agglomeration of the particles is observed after milling for a long duration of around 50 hrs. As the content of NaCl is increased, there is a reduction in the particle size to around 400-600 nm and also the agglomeration is reduced which could be beneficial for thermoelectric applications. The removal of NaCl will result in the formation of pores or voids inside the grains.

Densification of powders

In order to stabilize the Fe_2VAl phase and to proceed with further analyses like the measurement of the thermoelectric quantities, the densification of the powders was done by spark plasma sintering (SPS). XRD analysis of the sintered samples with BPRs 10:1 and 13:1 is shown in Figures 4 and 5. The densified samples display no trace of additional peaks related to secondary phases and the ($L2_1$) Heusler phase is still observed after sintering.

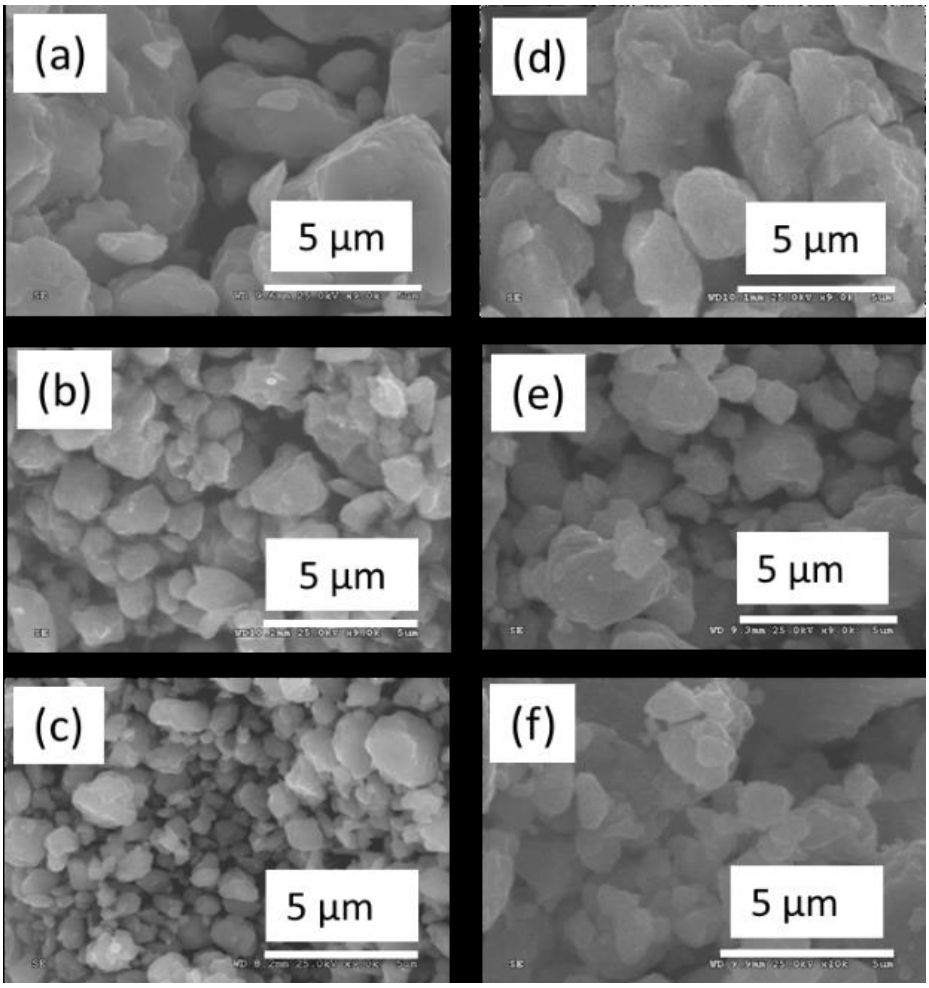

Figure 3: SEM analysis of milled Fe_2VAl powders BPR 10:1 (a) pure (c) 2 wt % NaCl, (c) 5 wt % NaCl, BPR 13:1 (d) pure, (e) 2 wt % NaCl, (f) 5 wt % NaCl.

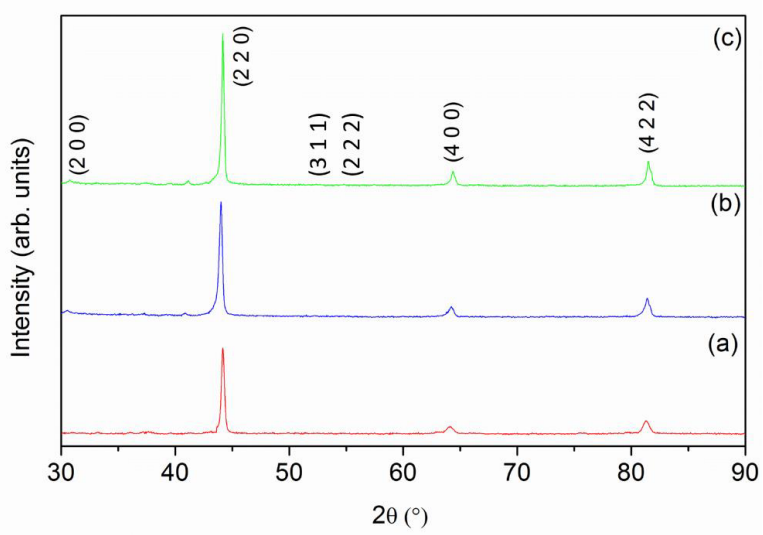

Figure 4: XRD patterns of sintered Fe_2VAl alloys with BPR 10:1 (a) Pure, (b) 2 wt % NaCl and (c) 5 wt % NaCl.

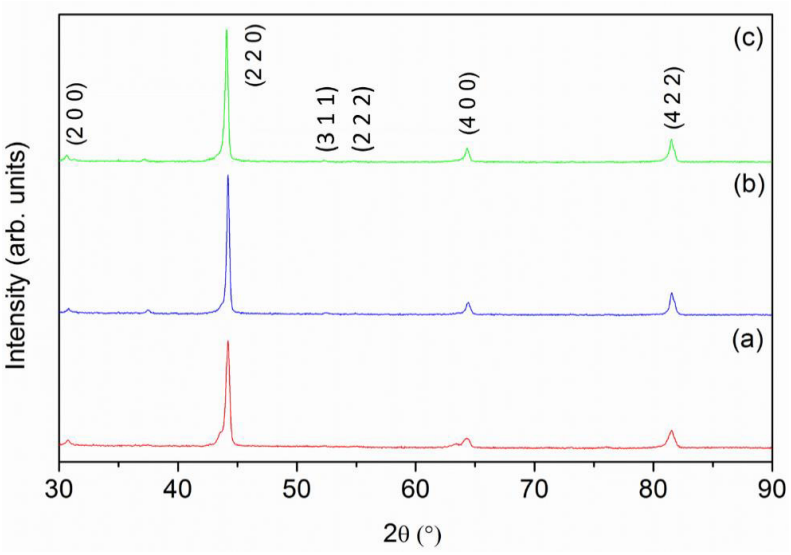

Figure 5: XRD patterns of sintered Fe_2VAl alloys with BPR 13:1 (a) Pure, (b) 2 wt % NaCl and (c) 5 wt % NaCl.

The morphology of the sintered samples is illustrated in Figure 6. The compositional analysis performed by EDXS indicates a pure Fe_2VAl phase in all the samples without any trace of unwanted secondary phases. The sintered samples, which were milled with NaCl, are found to be porous, which can clearly be seen in Figure 6. This porosity will help in the reduction of the thermal conductivity of the samples which will be presented in section 3.3.

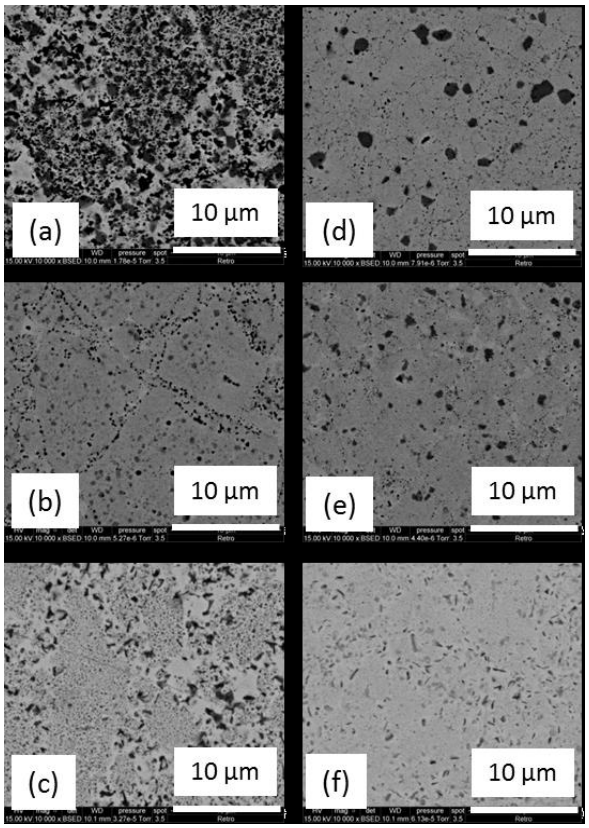

Figure 6: SEM analysis of sintered Fe_2VAl with BPR 10:1 (a) pure, (b) 2 wt % NaCl, (c) 5 wt % NaCl, BPR 13:1 (d) pure (e) 2 wt % NaCl, (f) 5 wt % NaCl.

To estimate the porosity, the density of the sintered alloys was measured by using Archimedes' principle. Figure 7 displays the relative density of the different samples, assuming the value of the theoretical density of Fe_2VAl, which is 6.59 g/cm^3, to be 100 %. The density of the samples is reduced to around 80 % of the theoretical density for the samples elaborated with BPRs 10:1 and 13:1 as the content of NaCl is increased during milling. The porosity of the samples is supposed to enhance thermoelectric properties by reducing the thermal conductivity value. However, one has to ensure that the reduction of the thermal conductivity is not accompanied by a reduction of the PF.

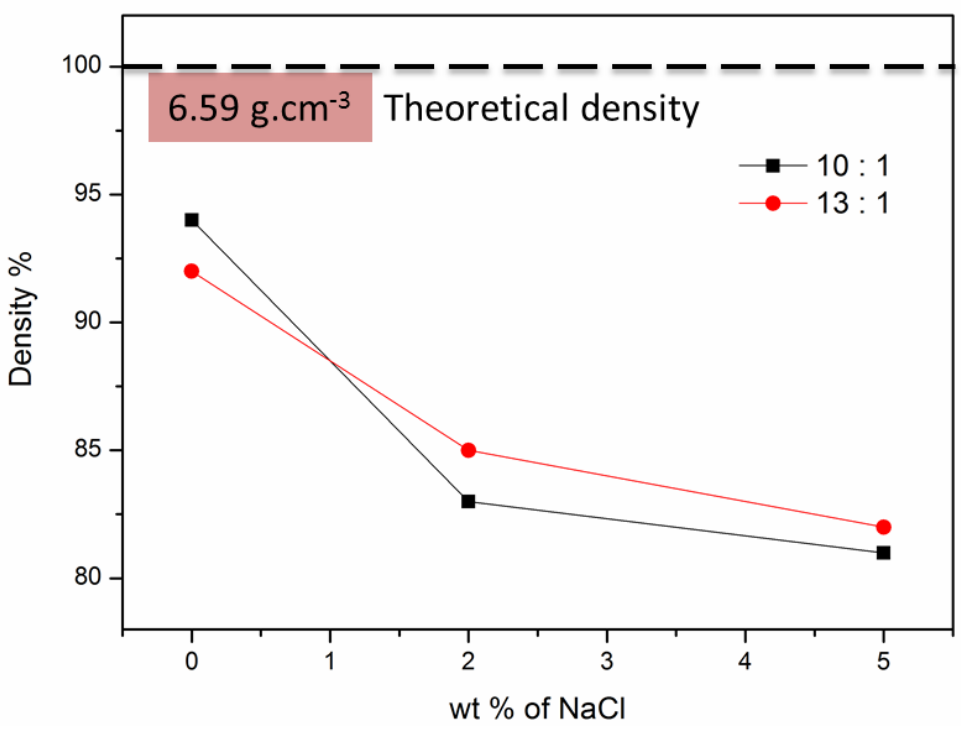

Figure 7: Relative Density fraction of sintered Fe_2VAl alloys.

Thermoelectric properties

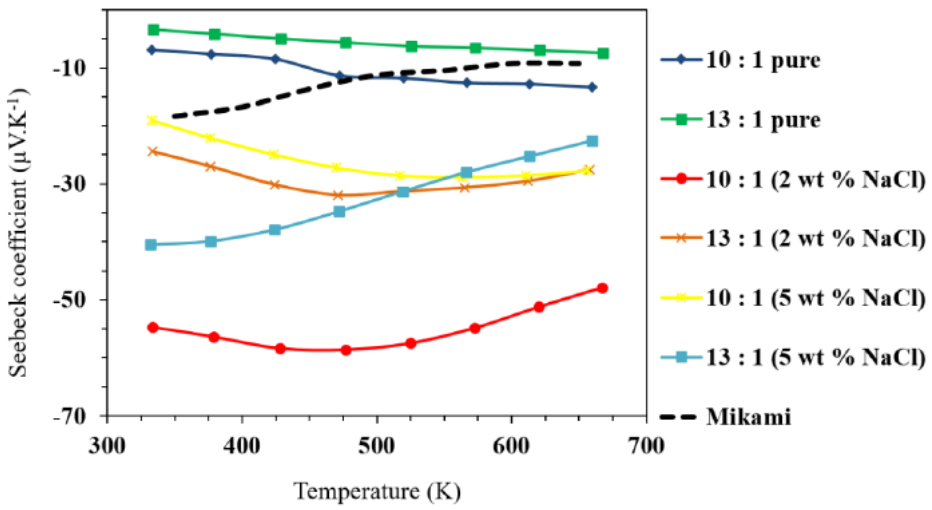

Figure 8: Temperature dependent Seebeck coefficient values of Fe_2VAl samples with and without porosity compared with the literature data [21].

The temperature dependence of the Seebeck coefficient is plotted in Figure 8. Even though Fe_2VAl is supposed to be a p-type material, our samples exhibit n-type conductivity. Nevertheless, the Seebeck coefficient values of Fe_2VAl without porosity are compared with the literature values of other ball-milled samples and are in good agreement with them [21]. The negative sign of the Seebeck coefficient might be the result of defects and disorder present in the synthesized samples. Moreover, the compositional analysis performed by EDXS shows the samples to be almost stoichiometric. This implies that the samples might be slightly disordered. Nonetheless, the influence of porosity is clearly seen on the values of the Seebeck coefficient. Addition of NaCl reduced the grain size of Fe_2VAl which could also be a main factor in the enhancement of the Seebeck coefficient. A similar kind of unusual behavior of the transport properties is also observed in Li doped Mg_2Ge which is justified by a non-rigid band structure approach [22]. In our case, the milling agent NaCl could cause a surface modification of the grains leading to carrier trapping. The porous samples with BPR 10:1 milled with 2 wt % NaCl with a porosity of around 17 % exhibit better values in comparison with the other samples.

The electrical resistivity measurements of the samples with respect to temperature are illustrated in Figure 9. It is quite obvious and expected that the resistivity values will increase with the porosity, which will result in the reduction of the electrical conductivity. This increase of the resistivity will be detrimental for the power factor but has to be compared with the increase of the Seebeck coefficient to see the global effect on the electronic properties.

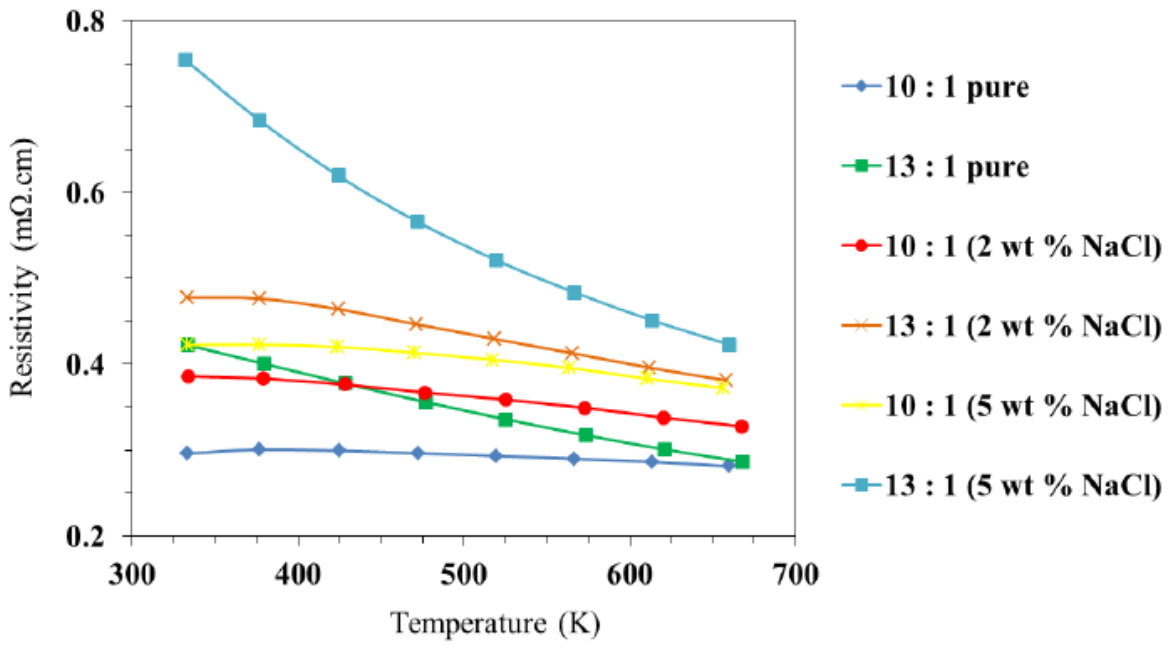

Figure 9: Resistivity values of Fe_2VAl samples as a function of temperature.

Figure 10 displays the PF values as a function of temperature. The PF values of the pure Fe_2VAl samples without any porosity are found to be very low. The magnitude of the PF is enhanced with the introduction of porosity in the samples. The samples milled with a 10:1 BPR and 2 wt % of NaCl, which are lowest in porosity among the porous samples, have the highest PF. In most cases, it is assumed that introducing porosity might degrade or enhance thermoelectric performance. Thus, it is important to note that a limited porosity is found to be beneficial to increase the PF.

The thermal conductivity values as a function of temperature are shown in Figure 11. The thermal conductivity has been reduced with the increase of porosity. A low value of the thermal conductivity around 5 $W.m^{-1}K^{-1}$ is obtained at room temperature. This reduction of κ can probably be attributed to the effect of phonon scattering at grain boundaries associated with the micropores in the microstructured sintered samples. Nevertheless, a more in-depth study (especially theoretical) is necessary to validate this assumption as well as to provide a clear explanation for the variation of the Seebeck coefficient.

Finally, the ZT values have been determined from the measured thermoelectric properties. Figure 12 portrays the ZT values as a function of temperature.

A significant increase in the ZT values is found by including porosity. A maximum ZT value of around 0.04 has been obtained at room temperature and a value of 0.07 at 550 K in the case of samples milled with a 10:1 BPR and with 2 wt% of NaCl. This can be attributed to the increase in the PF as well as to the reduction of the thermal conductivity shown earlier.

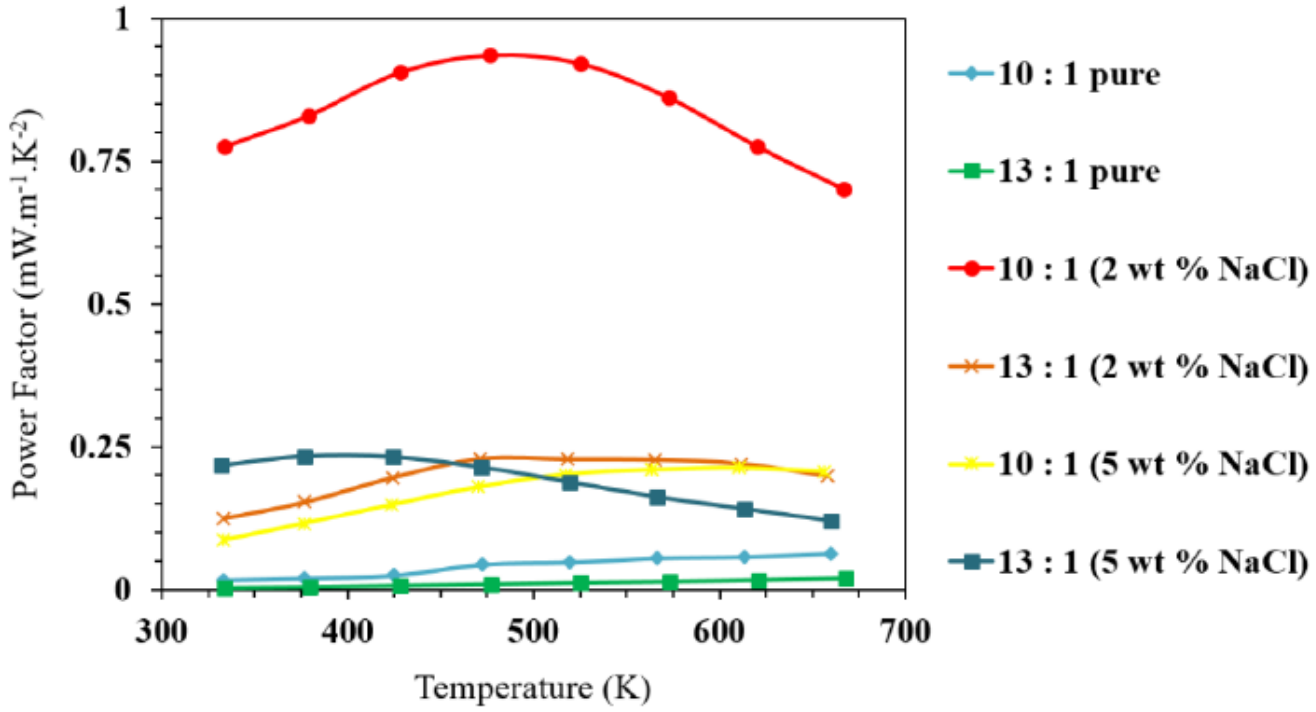

Figure 10: Power factor values of Fe_2VAl samples as a function of temperature.

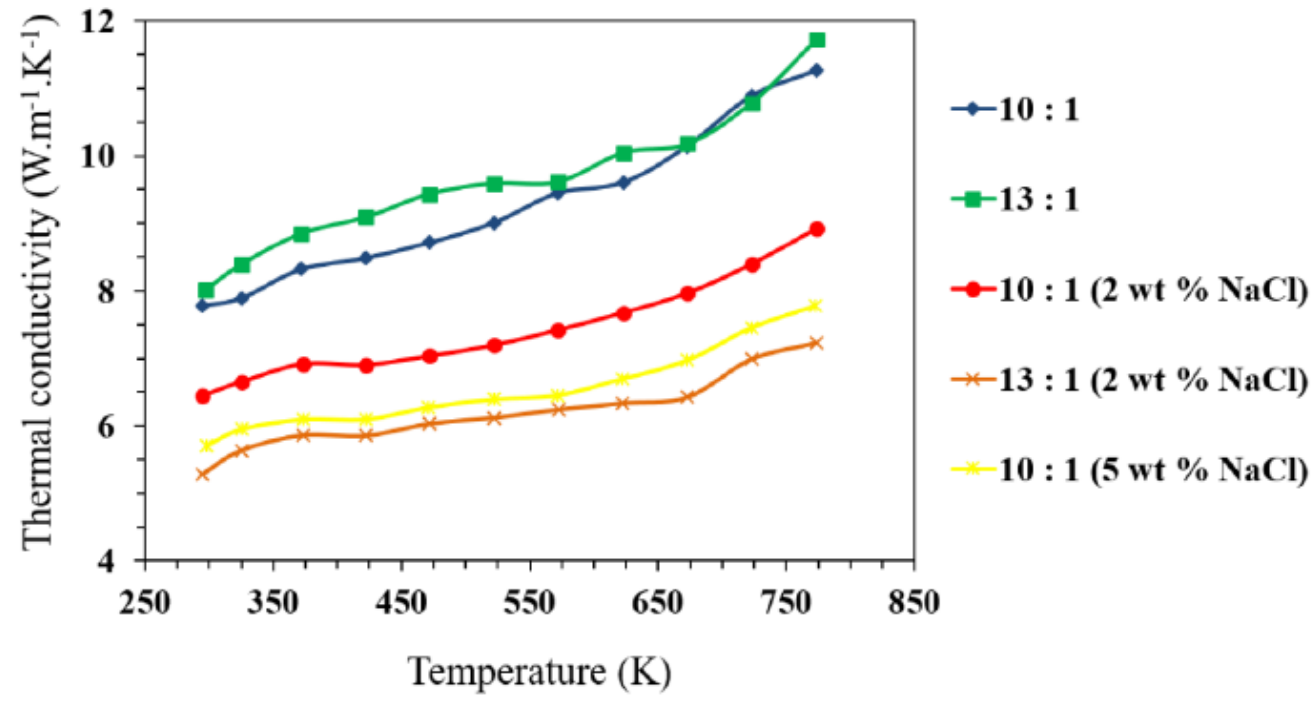

Figure 11: Thermal conductivity values of Fe_2VAl samples as a function of temperature.

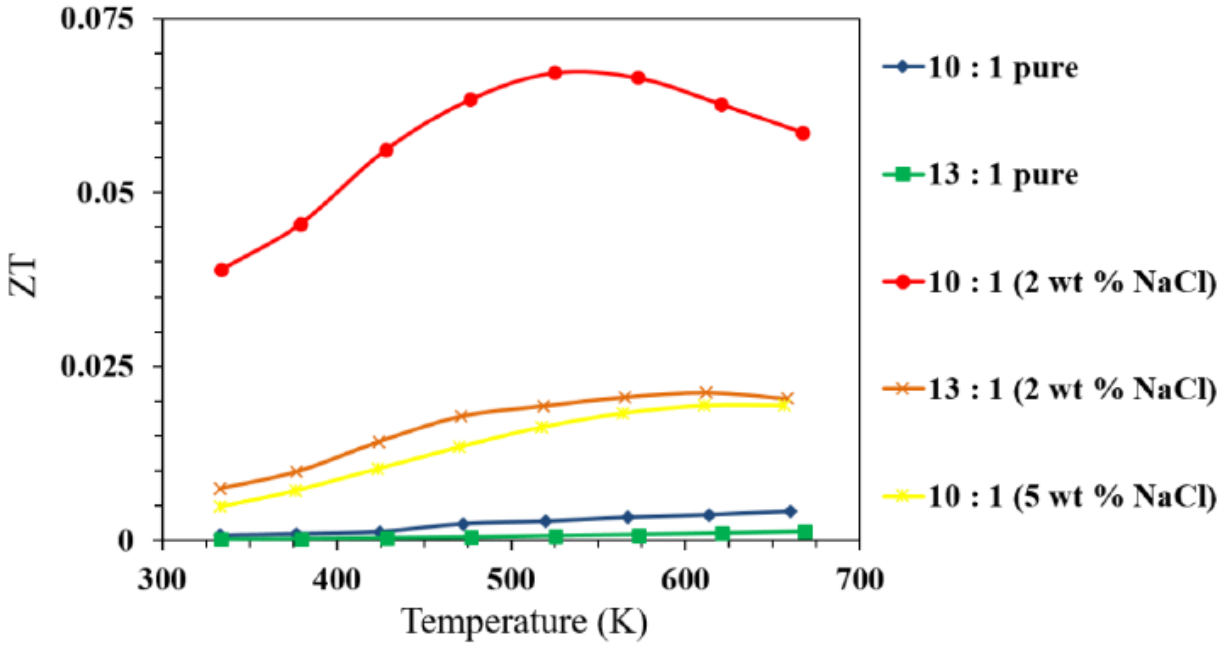

Figure 12: Temperature dependent ZT values of the porous Fe_2VAl alloys.

Conclusion

The method we have chosen to modify the microstructure and introduce porosity in Fe_2VAl samples has revealed itself to be quite successful. Around 20 % of porosity has been attained without any undesired phases irrespective of the BPR. The highest porosity has been reached with BPRs of 10:1 and 13:1 and 5 wt % of NaCl. The unusual enhancement in the Seebeck coefficient values of the samples milled with NaCl can come from the carrier trapping due to the use of milling agent or the formation of secondary phases. The samples milled with a 10:1 BPR and with 2 wt % of NaCl exhibit high Power Factors and low thermal conductivities leading to a significant enhancement of the ZT. Thus, it is important to note that the porosity has to be limited and controlled in order to obtain Fe_2VAl samples with good thermoelectric properties. So far, a clear explanation of these findings is still necessary and requires more in-depth analyses of the microstructure of the samples as well as a theoretical study of both the electronic and thermal properties of the porous samples containing NaCl. In our previous work, a theoretical analysis has already been performed to study the thermoelectric properties of Fe_2VAl with and without defects [23]. A significant enhancement of the thermoelectric efficiency is found in Al-rich $Fe_2V_{1-x}Al_{1+x}$ alloys. In a broader perspective, this work can be a starting step in the quest of various reagents to induce the optimized porosity and the desired defects without altering the actual Fe_2VAl phase.

Acknowledgement

We would like to thank Mr. Geoffroy Chevallier from PNF², CIRIMAT Toulouse for assistance in handling the SPS.

Conflict of Interest

No conflict of interest.

References

1. Pichanusakorn P, Bandaru P (2010) Nanostructured thermoelectrics. Materials Science and Engineering: R: Reports 67(2-4): 19-63.
2. Graf T, Felser C, Parkin SSP (2011) Simple rules for the understanding of Heusler compounds. Progress in Solid State Chemistry 39(1): 1-50.
3. Nishino Y, Kato M, Asano S, Soda K, Hayasaki M, et al. (1997) Semiconductor like Behavior of Electrical Resistivity in Heusler-type Fe_2VAl Compound. Physical Review Letters 79(10): 1909-1912.
4. Kato M, Nishino Y, Mizutani U, Asano S (2000) Electronic, magnetic and transport properties of $(Fe_{1-x}V_x)_3Al$ alloys. Journal of Physics: Condensed Matter 12(8): 1769.
5. Nishino Y (2000) Unusual electron transport in Heusler-type Fe_2VAl compound. Intermetallics 8(9): 1233-1241.
6. Nishino Y, Deguchi S, Mizutani U (2006) Thermal and transport properties of the Heusler-type $Fe_2VAl_{1-x}Ge_x$($0 \le x \le 0.20$) alloys: Effect of doping on lattice thermal conductivity, electrical resistivity, and Seebeck coefficient. Physical Review B 74(11): 115115.
7. Singh DJ, Mazin II (1998) Electronic structure, local moments, and transport in Fe_2VAl. Physical Review B 57(22): 14352-14356.
8. Guo GY, Botton GA, Nishino Y (1998) Electronic structure of possible 3d `heavy-fermion' compound Fe_2VAl. Journal of Physics: Condensed Matter 10(8): L119.
9. Weht R, Pickett WE (1998) Excitonic correlations in the intermetallic Fe_2VAl. Physical Review B 58(11): 6855-6861.

10. Bandaru S, Jund P (2016) Electronic structure of the Heusler compound Fe_2VAl and its point defects by ab initio calculations. physica status solidi (b) 254(2): 1600441.

11. Okamura H, Kawahara J, Nanba T, Kimura S, Soda K, et al. (2000) Pseudogap Formation in the Intermetallic Compounds $(Fe_{1-x}V_x)_3Al$. Physical Review Letters 84(16): 3674-3677.

12. Lue CS, Ross JH (1998) Semimetallic behavior in Fe_2VAl: NMR evidence. Physical Review B 58(15): 9763-9766.

13. Berche A, Noutack MT, Doublet ML, Jund P (2020) Unexpected band gap increase in the Fe_2VAl Heusler compound. Materials Today Physics 13: 100203.

14. Masashi M, Kobayashi K, Kawada T, Kubo K, Uchiyama N (2008) Development and Evaluation of High-Strength Fe_2VAl Thermoelectric Module. Japanese Journal of Applied Physics 47: 1512.

15. Lee H, Vashaee D, Wang DJ, Dresselhaus MS, Ren ZF, et al. (2010) Effects of nanoscale porosity on thermoelectric properties of SiGe. Journal of Applied Physics 107(9): 094308.

16. Lidorenko N (1970) Influence of Porosity and Intergrain-Boundary Quality on the Electrical and Thermal Conductivities of Semiconductive Thermoelectric Materials. Inorg Mat 6: 1853.

17. Liu R, Gao L, Li L, Zha X, Wang J, et al. (2017) Enhanced high-temperature thermoelectric performance of CdO ceramics with randomly distributed micropores. Journal of the American Ceramic Society 100(7): 3239-3245.

18. Kawaharada Y, Kurosaki K, Yamanaka S (2003) Thermophysical properties of Fe_2VAl. Journal of Alloys and Compounds 352(1-2): 48-51.

19. Mikami M, Kobayashi K, Kawada T, Kubo K, Uchiyama N (2009) Development of a Thermoelectric Module Using the Heusler Alloy Fe_2VAl. Journal of Electronic Materials 38(7): 1121-1126.

20. Mikami M, Kobayashi K (2008) Effect of Bi addition on microstructure and thermoelectric properties of Heusler Fe_2VAl-sintered alloy. Journal of Alloys and Compounds 466(1-2): 530-534.

21. Mikami M, Kinemuchi Y, Ozaki K, Terazawa Y, Takeuchi T (2012) Thermoelectric properties of tungsten-substituted Heusler Fe_2VAl alloy. Journal of Applied Physics 111(9): 093710.

22. Kamila H, Sankhla A, Yasseri M, Mueller E, de Boor J (2020) Non-Rigid Band Structure in Mg_2Ge for Improved Thermoelectric Performance. Advanced Science 7(12): 2000070.

23. Bandaru S, Katre A, Carrete J, Mingo N, Jund P (2017) Influence of Antisite Defects on the Thermoelectric Properties of Fe_2VAl. Nanoscale and Microscale Thermophysical Engineering 21(4): 237-246.